Tight-binding modeling of thermoelectric properties of bismuth telluride

Seungwon Lee[a] and Paul von Allmen
Jet Propulsion Laboratory, California Institute of Technology, Pasadena, California 91109

(Received 11 October 2005; accepted 9 December 2005; published online 10 January 2006)

A parameterized orthogonal tight-binding model with $sp^3d^5s^*$ orbitals, nearest-neighbor interactions, and spin-orbit coupling is developed for bismuth telluride (Bi_2Te_3) and used to study its thermoelectric properties. Thermoelectric transport coefficients and figures of merit for *n*-doped and *p*-doped Bi_2Te_3 are calculated by solving Boltzmann's transport equation within the constant-relaxation-time approximation. The dependence of the computed thermoelectric figure of merit on the electrical conductivity is in good agreement with experiment. The parameterized tight-binding model serves as a basis for studies of confined Bi_2Te_3 systems in search of enhanced thermoelectric properties. © *2006 American Institute of Physics*. [DOI: 10.1063/1.2162863]

Bismuth telluride (Bi_2Te_3) is a material of particular interest for thermoelectric applications. It is one of the best bulk materials in terms of the thermoelectric figure of merit *ZT*.[1] It has been theoretically predicted and experimentally demonstrated that confined Bi_2Te_3 systems such as quantum wires/wells exhibit an even larger *ZT* thanks to enhanced thermoelectric power and electrical conductivity or reduced thermal conductivity.[2–6] These initial results have triggered considerable effort in fabricating the confined systems and finding the geometries for optimal thermoelectric properties.[7–10] Fabrication methods for a stable and predictable geometry of such a confined system are progressing and will enable a wide exploration of the design space. This motivates a need for thermoelectric-material modeling tools that can help guide the selection of the geometry of the confined system with the largest *ZT*.

Most existing theoretical studies for the thermoelectric properties of low-dimensional structures use continuum models (e.g., effective mass approximation) because of their computational efficiency.[2,3,11–16] However, continuum models cannot take into account atomic-level effects due to, for example, interface states in quantum-wire/well superlattices and surface states in quantum wires/wells. On the other hand, most *ab initio* models, which are atomistic by definition, do not scale well in terms of computational time as the number of atoms involved increases. Parameterized tight-binding models bridge the gap between the poorly scalable atomistic models and the scalable nonatomistic models. The tight-binding model is atomistic, yet computationally efficient due to the reduced number of basis orbitals and the flexible parameterization of the Hamiltonian.

To date, there has been only one study about the tight-binding modeling of Bi_2Te_3, using a sp^3-orbital nearest-neighbor orthogonal model.[17] This simple model was applied to qualitatively understand the main features of the density of states and chemical bonding in Bi_2Te_3. However, the tight-binding model cannot quantitatively describe the electronic structure and thermoelectric properties of Bi_2Te_3. In this letter, a parameterized tight-binding model for Bi_2Te_3 is developed with good accuracy in describing the electronic structures and applied to study thermoelectric properties.

[a]Electronic mail: seungwon.lee@jpl.nasa.gov

Considering a trade-off between model accuracy and computational efficiency, an orthogonal tight-binding model with $sp^3d^5s^*$ orbitals, nearest-neighbor interactions, and spin-orbit coupling is chosen. Bi_2Te_3 contains five atoms in the primitive cell (Te^I–Bi–Te^{II}–Bi–Te^I).[18] Although Te^I and Te^{II} are the same type of atom, their neighbors are different: the nearest neighbors of Te^I are three Te atoms and three Bi atoms, while those of Te^{II} are six Bi atoms. To capture the difference, separate tight-binding parameters are assigned to Te^I and Te^{II}. This leads to a total of 71 independent parameters in the tight-binding model.

The tight-binding parameters are determined by fitting the computed band structure to a first-principles band structure obtained with a screened-exchange local density approximation.[19] The first-principles band structure predicts the energy gap, the degeneracy of the conduction and valence band edges, and the effective masses of the two bands, in good agreement with experimental results.[19] In the fitting process, a higher priority is given to the highest valence and the lowest conduction bands than to the rest of the band structure, since these two bands are mainly responsible for the thermoelectric properties of lightly doped Bi_2Te_3. Moreover, the locations, energies, and effective masses of the two band edges are emphasized, as they largely determine the model accuracy for thermoelectric properties. In order to ensure that the band edges are located at the target *k* point, 8000 *k* points are sampled in the first Brillouin zone. The resulting tight-binding parameters are listed in Table I, and the fitting accuracy for the key target values is listed in Table II. Overall, a fitting accuracy within 5% was achieved.

The band structure obtained with the fitted tight-binding parameters is plotted in Fig. 1 in comparison with the target band structure from the first-principles calculation. The overall shapes of the highest valence band and the lowest conduction band are in good agreement with the target. The degeneracies of the band edges are also accurately reproduced in the fitted band structure. Note that the band edges are not located along the high-symmetry lines, but rather off the symmetry line in the reflection planes.[19] Figure 2 shows the energy contours of the highest valence band and the lowest conduction band in the *y*-*z* reflection plane. The band edges are denoted by valence band edge (VBE) and conduction band edge (CBE). The valence band contour exhibits an elongated pocket, while the conduction band contour shows

TABLE I. Tight-binding parameters for Bi_2Te_3 using an $sp^3d^5s^*$-orbitals nearest-neighbor orthogonal model with spin-orbit coupling. Bi_2Te_3 has a layered primitive cell containing five atoms: Te^I–Bi–Te^{II}–Bi–Te^I. The energy zero is taken at the top of the valence band. The energies are in units of electron-volts.

	Bi	Te^I	Te^{II}
E_s	−9.0657	−10.2050	−10.9796
E_p	2.0431	−0.5410	−1.3313
E_d	18.0680	12.5410	10.2980
E_{s^*}	8.2718	14.2024	14.1324
λ_{so}	0.8982	0.2362	0.4326	
	(Bi, Te^I)	(Bi, Te^{II})	(Te^I, Te^I)
$ss\sigma$	−0.3735	−0.6797	−0.3402
$s^*s^*\sigma$	−0.4424	−0.6857	−1.3463
$ss^*\sigma$	−0.6194	−0.0010	−0.0011
$s^*s\sigma$	−0.0010	−0.1268	−0.0011
$sp\sigma$	1.8234	0.7972	0.5896
$ps\sigma$	1.0165	0.4921	0.5896
$s^*p\sigma$	1.2503	0.0011	0.7384
$ps^*\sigma$	0.6406	0.4653	0.7384
$sd\sigma$	−0.7240	−1.0984	−0.5926
$ds\sigma$	−1.1863	−0.9489	−0.5926
$s^*d\sigma$	−0.1250	−0.0378	−1.0654
$ds^*\sigma$	−0.0010	−0.6360	−1.0654
$pp\sigma$	2.2860	1.6122	1.1292
$pp\pi$	−0.6192	−0.4125	−0.0010
$pd\sigma$	−1.8266	−1.8716	−1.5154
$dp\sigma$	−1.4842	−0.6893	−1.5154
$pd\pi$	0.4966	1.1729	1.9631
$dp\pi$	1.4372	1.1182	1.9631
$dd\sigma$	−1.2178	−1.3396	−1.4381
$dd\pi$	2.1665	2.6219	2.5731
$dd\delta$	−0.0953	−1.2809	−1.4284

a more isotropic pocket. These shapes are in good agreement with the target band structure.[19]

The parameterized tight-binding model is applied to study the thermoelectric properties of Bi_2Te_3. Although more sophisticated models are available to realistically treat carrier scattering processes,[15,20–22] a constant-relaxation-time approximation is chosen as an initial step to validate our parameterized tight-binding model for thermoelectric modeling. The semiclassical approach has been widely taken within both continuum models and first-principles

TABLE II. Fitting accuracy of the tight-binding parameters. The locations of the conduction and valence band edges (k_{CBE} and k_{VBE}) are given in the basis set of the reciprocal primitive vectors. The energy gap (E_{gap}) is given in units of electron volts, and the electron and hole effective masses (m^e and m^h) along the x,y,z directions are given in units of the free electron mass.

	Target	Fitted	Deviation (%)
k_{CBE}	[0.65,0.55,0.55]	[0.65,0.56,0.56]	[1.1,5.0,5.0]
k_{VBE}	[0.55,0.40,0.40]	[0.54,0.38,0.38]	[1.1,1.3,1.3]
E_{gap}	0.154	0.158	2.6
m^e_{xx}	0.019	0.019	0.8
m^e_{yy}	0.125	0.125	0.004
m^e_{zz}	0.137	0.132	3.6
m^h_{xx}	0.025	0.025	0.1
m^h_{yy}	0.263	0.262	0.4
m^h_{zz}	0.192	0.201	4.7

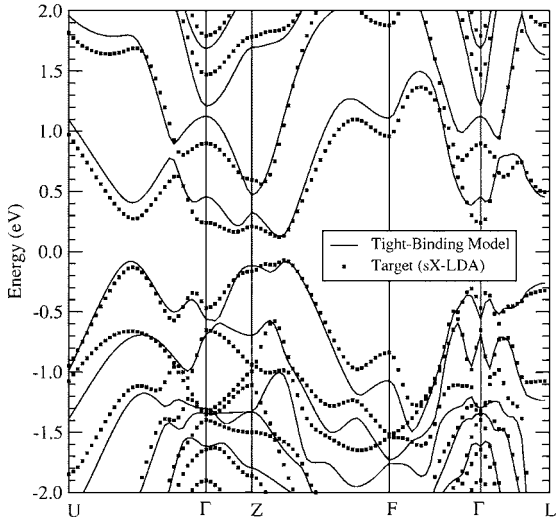

FIG. 1. Tight-binding band structure compared with the target band structure from a screened-exchange local density approximation calculation in Ref. 19.

calculations.[2,3,13,14,16,23] A solution to Boltzmann's transport equation in the constant-relaxation-time approximation leads to the following expressions for the electrical conductivity tensor σ, the electronic thermal conductivity κ_e, and the Seebeck coefficient S:

$$\sigma = \Lambda^{(0)}, \tag{1}$$

$$\kappa_e = \frac{1}{e^2T}[\Lambda^{(2)} - \Lambda^{(1)}(\Lambda^{(0)})^{-1}\Lambda^{(1)}], \tag{2}$$

$$S = \frac{1}{eT}(\Lambda^{(0)})^{-1}\Lambda^{(1)}, \tag{3}$$

$$\Lambda^{(\alpha)}_{mn} = e^2\tau \int \frac{d^3k}{4\pi^3}\left(-\frac{\partial f}{\partial \epsilon}\right) v_m(k)v_n(k)[\epsilon(k) - \mu]^\alpha, \tag{4}$$

where e is the charge of the carriers, T is the temperature, $\epsilon(k)$ is the energy associated with wave vector k, $f(\epsilon)$ is the Fermi distribution function, τ is the relaxation time for the scattering term in Boltzmann's equation, $v(k)$ is the group velocity associated with wave vector k, and μ is the chemical potential.

To evaluate the transport coefficients, the energy and group velocity for each wave vector are calculated within the present tight-binding model. For the integration over the first Brillouin zone, over 180 000 k points are sampled on a uniform rectangular grid to ensure the convergence of the integral within 1%. A constant relaxation time is determined by fitting to the experimental data for the Seebeck coefficient variation with respect to the electrical conductivity.[1] Note that the electronic thermal conductivity is not involved in this process of determining the relaxation time. A relaxation time of 2.2×10^{-14} s gives a good agreement for n-doped Bi_2Te_3 and 5.5×10^{-15} s for p-doped Bi_2Te_3. Using the calculated values for σ, S, and κ_e and the experimental values for the lattice thermal conductivity ($\kappa_{ph}=1.5$ Wm^{-1} K^{-1}),[1] the thermoelectic figure of merit $ZT=\sigma S^2T/(\kappa_e+\kappa_{ph})$ at 300 K is computed.

The components along the basal plane of the resulting σ, S, κ_e, and ZT are plotted in Fig. 3. As the electrical conduc-

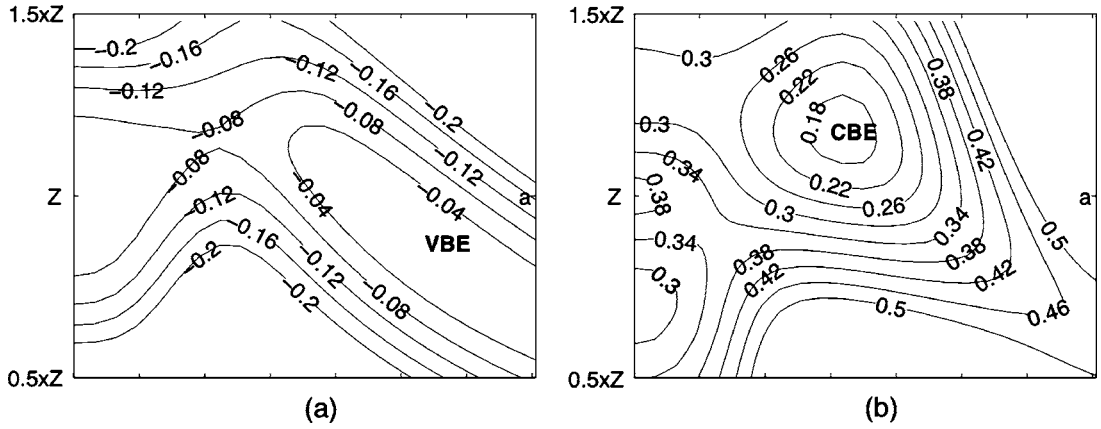

FIG. 2. Contour plots of the energies of (a) the highest valence band and (b) the lowest conduction band in the y-z plane, where $Z=[0.5,0.5,0.5]$ and $a=[0.641,0.430,0.430]$ in the basis set of the reciprocal primitive vectors. The locations of the valence (VBE) and conduction (CBE) band edges are marked at [0.543, 0.381, 0.381] and [0.653, 0.556, 0.556], respectively.

tivity approaches the intrinsic value, the Seebeck coefficient decreases to zero and the electronic thermal conductivity increases. The values of $\kappa_{e(xx)}$, the component along the basal plane of κ_e, are comparable to the lattice thermal conductivity. The estimated values of ZT with respect to σ are in good agreement with experiment.[1] Note that although σS^2 in ZT is implicitly fitted to the experiment through the adjustment of the relaxation time, κ_e is not fitted. The good agreement between the computed and experimental ZT shows that our model describes the electronic transport properties with reasonable accuracy.

In conclusion, a parameterized orthogonal tight-binding model with $sp^3d^5s^*$ orbitals, nearest-neighbor interactions, and spin-orbit coupling is developed for Bi_2Te_3 and used to study the thermoelectric properties within the constant-relaxation-time approximation. The computed properties are in good agreement with experiment in terms of not only the general trend but also the quantitative values. Future work includes more realistic modeling of electronic transport properties through a full solution to Boltzmann's equation with representative scattering mechanisms and tight-binding modeling of confined Bi_2Te_3 systems in search of enhanced thermoelectric properties.

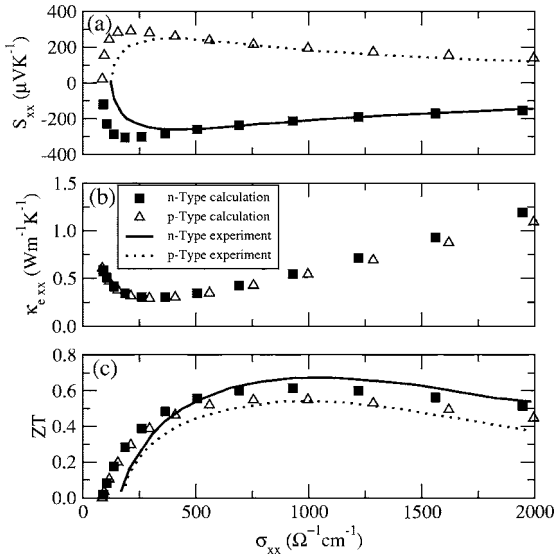

FIG. 3. Thermoelectric properties calculated with the parameterized tight-binding model and the constant relaxation time approximation for n-doped and p-doped Bi_2Te_3 along the basal plane. The thermoelectric power S_{xx}, the electronic thermal conductivity $\kappa_{e(xx)}$, and the thermoelectric figure of merit ZT are plotted with respect to the electrical conductivity σ_{xx}, and they are compared with experimental data from Ref. 1.

The authors would like to thank Miyoung Kim and Arthur J. Freeman for providing their first-principles band structure calculations which were used for the tight-binding model parameter fitting. This work was carried out at Jet Propulsion Laboratory, California Institute of Technology under a contract with the National Aeronautics and Space Administration. This work was supported by a grant from the Defense Advanced Research Projects Agency.

[1] H. J. Goldsmid, *Thermoelectric Refrigeration* (Plenum, New York, 1964).
[2] L. D. Hicks and M. S. Dresselhaus, Phys. Rev. B **47**, 12727 (1993).
[3] L. D. Hicks and M. S. Dresselhaus, Phys. Rev. B **47**, 16631 (1993).
[4] F. J. DiSalvo, Science **285**, 703 (1999).
[5] R. Venkatasubramanian, E. Siivola, T. Colpitts, and B. O'Quinn, Nature (London) **413**, 597 (2001).
[6] A. Balandin and K. L. Wang, Phys. Rev. B **58**, 1544 (1998).
[7] Y. Xia, P. Yang, Y. Sun, Y. Wu, B. Mayers, B. Gates, Y. Yin, F. Kim, and H. Yan, Adv. Mater. (Weinheim, Ger.) **15**, 353 (2003).
[8] J. R. Lim, J. F. Whitacre, J.-P. Fleurial, C.-K. Huang, M. A. Ryan, and N. V. Myung, Adv. Mater. (Weinheim, Ger.) **17**, 1488 (2005).
[9] X. B. Zhao, X. H. Ji, Y. H. Zhang, T. J. Zhu, J. P. Tu, and X. B. Zhang, Appl. Phys. Lett. **86**, 062111 (2005).
[10] E. J. Menke, Q. Li, and R. M. Penner, Nano Lett. **4**, 2009 (2004).
[11] X. Sun, Z. Zhang, and M. S. Dresselhaus, Appl. Phys. Lett. **74**, 4005 (1999).
[12] O. Rabin, Y.-M. Lin, and M. S. Dresselhause, Appl. Phys. Lett. **79**, 81 (2001).
[13] D. A. Broido and T. L. Reinecke, Phys. Rev. B **51**, 13797 (1995).
[14] D. A. Broido and T. L. Reinecke, Appl. Phys. Lett. **67**, 100 (1995).
[15] D. A. Broido and T. L. Reinecke, Phys. Rev. B **64**, 045324 (2001).
[16] J. O. Sofo and G. D. Mahan, Appl. Phys. Lett. **65**, 2690 (1994).
[17] P. Pecheur and G. Toussaint, Phys. Lett. A **135**, 223 (1989).
[18] *Semiconductors: Data Handbook* 3rd ed., edited by O. Madelung (Springer, Berlin, 2004).
[19] M. Kim, A. J. Freeman, and C. B. Geller, Phys. Rev. B **72**, 035205 (2005).
[20] B. A. Sanborn, P. B. Allen, and G. D. Mahan, Phys. Rev. B **46**, 15123 (1992).
[21] J. O. Sofo and G. D. Mahan, Phys. Rev. B **49**, 4565 (1994).
[22] P. J. Lin-Chung and A. K. Rajagopal, Phys. Rev. B **60**, 12033 (1999).
[23] T. J. Scheidemantel, C. Ambrosch-Draxl, T. Thonhauser, J. V. Badding, and J. O. Sofo, Phys. Rev. B **68**, 125210 (2003).